

BNL-64628  
 PRINCETON/HEP/97-10  
 TRI-PP-97-26  
 KEK Preprint 97-113

## Observation of the Decay $K^+ \rightarrow \pi^+ \gamma \gamma$

P. Kitching, T. Nakano<sup>(a)</sup>, M. Rozon<sup>(b)</sup>, and R. Soluk

*Centre for Subatomic Research, University of Alberta, Edmonton, Alberta, Canada, T6G 2N5*

S. Adler, M.S. Atiya, I-H. Chiang, J.S. Frank, J.S. Haggerty, T.F. Kycia, K.K. Li,  
 L.S. Littenberg, A. Sambamurti<sup>(c)</sup>, A. Stevens, R.C. Strand, and C. Witzig

*Brookhaven National Laboratory, Upton, New York 11973*

W.C. Louis

*Medium Energy Physics Division, Los Alamos National Laboratory,  
 Los Alamos, New Mexico 87545*

D.S. Akerib<sup>(d)</sup>, M. Ardebili<sup>(e)</sup>, M. Convery<sup>(f)</sup>, M.M. Ito<sup>(g)</sup>, D.R. Marlow,  
 R.A. McPherson<sup>(h)</sup>, P.D. Meyers, M.A. Selen<sup>(i)</sup>, F.C. Shoemaker, and A.J.S. Smith

*Joseph Henry Laboratories, Princeton University, Princeton, New Jersey 08544*

E.W. Blackmore, D.A. Bryman, L. Felawka, A. Konaka, Y. Kuno<sup>(j)</sup>, J.A. Macdonald,  
 T. Numao, P. Padley<sup>(k)</sup>, J.-M. Poutissou, R. Poutissou, J. Roy<sup>(l)</sup>, and A.S. Turcot<sup>(m)</sup>

*TRIUMF, Vancouver, British Columbia, Canada, V6T 2A3*

(August, 1997)

## Abstract

The first observation of the decay  $K^+ \rightarrow \pi^+ \gamma \gamma$  is reported. A total of 31 events was observed with an estimated background of  $5.1 \pm 3.3$  events in the  $\pi^+$  momentum range from 100 MeV/c to 180 MeV/c. The corresponding partial branching ratio,  $B(K^+ \rightarrow \pi^+ \gamma \gamma, 100 \text{ MeV}/c < P_{\pi^+} < 180 \text{ MeV}/c)$ , is  $(6.0 \pm 1.5\{\text{stat}\} \pm 0.7\{\text{sys}\}) \times 10^{-7}$ . No  $K^+ \rightarrow \pi^+ \gamma \gamma$  decay was observed in the  $\pi^+$  momentum region greater than 215 MeV/c. The observed  $\pi^+$  momentum spectrum is compared with the predictions of chiral perturbation theory.

PACS numbers: 13.20.Eb, 12.39.Fe

Typeset using REVTeX

We report the first observation of the rare decay  $K^+ \rightarrow \pi^+\gamma\gamma$ . This decay provides a stringent test of chiral perturbation theory (ChPT) [1] since there is no tree-level  $O(p^2)$  contribution and the leading contributions start at  $O(p^4)$  [2]. It includes one undetermined coupling constant,  $\hat{c}$ , at  $O(p^4)$  for which various models predict different values of order of 1 ( $O(1)$ ) [3–6]. Both the branching ratio and the spectrum shape of  $K^+ \rightarrow \pi^+\gamma\gamma$  are sensitive to  $\hat{c}$ , and the total branching ratio is predicted to be  $(0.4 - 1) \times 10^{-6}$  for  $\hat{c}$  of  $O(1)$ . Measurements of  $K_L \rightarrow \pi^0\gamma\gamma$  [7,8] indicate the necessity for next-to-leading order ( $O(p^6)$ ) “unitarity” corrections [9,10] which can be deduced from an empirical fit of the decay amplitude of  $K_L \rightarrow \pi^+\pi^-\pi^0$ . Similar corrections for  $K^+ \rightarrow \pi^+\gamma\gamma$  from  $K^+ \rightarrow \pi^+\pi^-\pi^+$  predict a 30–40% higher branching ratio than the  $O(p^4)$  calculations with  $\hat{c} \sim O(1)$  [11]. From the measurement of the branching ratio and spectrum shape of  $K^+ \rightarrow \pi^+\gamma\gamma$ , it is possible to determine a value of  $\hat{c}$  and also to examine whether the unitarity corrections are necessary. Observation of this decay mode in excess of the Standard Model rate would suggest the existence of new phenomena such as sequential decays of the form  $K^+ \rightarrow \pi^+X^0, X^0 \rightarrow \gamma\gamma$ , where  $X^0$  is a massive short-lived neutral scalar particle. Our previous search [12] for  $K^+ \rightarrow \pi^+\gamma\gamma$  was confined to the region of phase space with  $P_{\pi^+} > 215$  MeV/c. We obtained a 90% C.L. upper limit on  $B(K^+ \rightarrow \pi^+\gamma\gamma)$  of  $10^{-6}$  when a constant matrix element (phase-space distribution) was assumed, but only  $10^{-3}$ – $10^{-4}$  when the ChPT spectrum with  $\hat{c} \sim O(1)$  was assumed. The present work expands the search to include the region  $P_{\pi^+} < 180$  MeV/c which is favored by ChPT.

The E787 setup at the Brookhaven Alternating Gradient Synchrotron has been described in detail in Ref. [13]. An 800-MeV/c kaon beam was slowed by a BeO degrader and stopped in a segmented scintillating fiber target located at the center of the detector. Charged decay products were momentum-analyzed in a cylindrical drift chamber placed in a 1-T solenoidal magnetic field. Their kinetic energy and range were measured by using the target and a 15-layer plastic scintillator (range stack) which surrounded the drift chamber. Signals from the range stack were fed to 500 MHz transient digitizers (TD) in order to identify the  $\pi^+ \rightarrow \mu^+ \rightarrow e^+$  decay chain in the stopping layer. Photons were detected in a lead-scintillator barrel calorimeter surrounding the range stack. The barrel calorimeter had 48-fold azimuthal and 4-fold radial segmentation with a total thickness of 14 radiation lengths. It covered a solid angle of about  $3\pi$  sr. Most of the remaining solid angle in the end regions was covered by 12-radiation-length end-cap calorimeters located upstream and downstream of the drift chamber.

To avoid background from the two-body decay  $K^+ \rightarrow \pi^+\pi^0$  ( $K_{\pi 2}$ ) with a 21% branching ratio and a monochromatic  $\pi^+$  momentum of 205 MeV/c ( $K_{\pi 2}$  peak), we searched for the  $K^+ \rightarrow \pi^+\gamma\gamma$  decay in the regions above the  $K_{\pi 2}$  peak,  $P_{\pi^+} > 215$  MeV/c ( $\pi\gamma\gamma 1$  region), and below the peak,  $100$  MeV/c  $< P_{\pi^+} < 180$  MeV/c ( $\pi\gamma\gamma 2$  region). To select  $K^+ \rightarrow \pi^+\gamma\gamma$  candidates, multilevel triggers followed a threefold strategy: (1) a  $K^+$  must stop in the target; (2) the decay particle must penetrate into the range stack with the range longer ( $\pi\gamma\gamma 1$ ) or shorter ( $\pi\gamma\gamma 2$ ) than that of a  $\pi^+$  from  $K_{\pi 2}$ , and be identified as a  $\pi^+$ ; and (3) the number of photon clusters in the barrel calorimeter must be exactly two with two-photon invariant mass ( $m_{\gamma\gamma}$ ) smaller ( $\pi\gamma\gamma 1$ ) or larger ( $\pi\gamma\gamma 2$ ) than the  $\pi^0$  mass. The  $\pi\gamma\gamma 1$  trigger which satisfied the above strategy was achieved by modifying the logic described in Ref. [12] to reject events with photons showering in the end-cap calorimeters and events with  $m_{\gamma\gamma}$  greater than 130 MeV/c<sup>2</sup> ( $P_{\pi^+} = 207$  MeV/c). For the search in the  $\pi\gamma\gamma 2$  region,

requirements in addition to the beam and range conditions at the first trigger level were (i) a large energy deposit ( $\sim 190$  MeV) in the barrel calorimeter and (ii) the large  $\gamma\text{--}\gamma$  opening angle ( $\theta_{\gamma\gamma} > 75^\circ$ ) so as to reduce  $K_{\pi 2}$  background. At the second trigger level, the on-line TD requirement to identify the  $\pi^+ \rightarrow \mu^+ \nu_\mu$  decay [12] was removed to avoid an unnecessary acceptance loss. At the third trigger level,  $m_{\gamma\gamma}$  was calculated, and an event was rejected if  $m_{\gamma\gamma} < 190$  MeV/ $c^2$  ( $P_{\pi^+} = 183$  MeV/ $c$ ). From the data taken in 1991, the total number of stopped kaons was  $3.1 \times 10^{10}$  for the  $\pi\gamma\gamma 1$  trigger and  $6.1 \times 10^{10}$  for the  $\pi\gamma\gamma 2$  trigger. The difference between the two  $K^+$  counts was mainly due to a hardware prescale factor of 2 applied to the  $\pi\gamma\gamma 1$  trigger. A total of  $7.3 \times 10^5$  events survived the  $\pi\gamma\gamma 1$  trigger, and  $2.7 \times 10^6$  events survived the  $\pi\gamma\gamma 2$  trigger.

For the off-line search in the  $\pi\gamma\gamma 1$  region [14], we required unambiguous identification of a single charged track as a  $\pi^+$  by measuring its range, energy and momentum, and by observing the  $\pi^+ \rightarrow \mu^+$  decay. Adjacent hit modules in the barrel calorimeter were grouped to identify two isolated photon showers (clusters). The hit position in each module along the beam axis ( $z$ ) was calculated from the end-to-end time and energy differences. The azimuthal angle ( $\phi$ ) of the hit position was determined up to the segmentation of the modules. Then, the location of the photon shower in  $z$  and  $\phi$  was obtained by an energy-weighted average of the hit positions. Events were rejected if the photon-pair opening angle and an energy of either the high or low energy photon were consistent with  $K^+ \rightarrow \pi^+ \pi^0$ ,  $\pi^0 \rightarrow \gamma\gamma$  kinematics. Cuts were applied on the photon energy ratio and opening angle to remove events which could be affected by fluctuations in visible energy or by accidentals. Finally, the remaining events were tested by a constrained kinematic fit for consistency with  $K^+ \rightarrow \pi^+ \gamma\gamma$ . The constraints included total momentum and energy conservation and consistency of the charged track's energy, momentum and range with a pion hypothesis. Events that had a  $\chi^2$  confidence level,  $P(\chi^2)$ , greater than 0.1 were accepted. No event was seen in the region of  $E_{\pi^+} > 117$  MeV/ $c^2$ , or equivalently  $P_{\pi^+} > 215$  MeV/ $c$ .

The analysis for the  $\pi\gamma\gamma 2$  region followed procedures mostly similar to those of the  $\pi\gamma\gamma 1$  analysis with the following differences. The major background sources in the  $\pi\gamma\gamma 2$  region are the  $K^+ \rightarrow \pi^+ \pi^0 \pi^0$  ( $K_{\pi 3}$ ) and  $K^+ \rightarrow \pi^+ \pi^0 \gamma$  ( $K_{\pi 2\gamma}$ ) decays with escaping or overlapping photons; these channels do not involve muons in the decay products. This allowed removal of the  $\pi^+ \rightarrow \mu^+$  tagging condition in order to increase the acceptance by more than a factor of 2. Since there was a large correlation between the measured energy and range for a low energy  $\pi^+$ , the range-momentum relation was removed from the constraints of the kinematic fit. Photon vetoes were tightened to reject  $K_{\pi 3}$  and  $K_{\pi 2\gamma}$  events with escaping photons. A cut was placed on the angle between the  $\pi^+$  and the higher-energy photon ( $\theta_{\pi^+\gamma_1}$ ) to remove events with a highly asymmetric photon-pair decay. Events were rejected if  $\cos \theta_{\pi^+\gamma_1} < -0.8$ . This cut also reduced  $K_{\pi 2\gamma}$  events with the radiative photon overlaying one of the two photons from  $\pi^0$  decay. Since the radiative photon from  $K_{\pi 2\gamma}$  was preferentially aligned along the  $\pi^+$  direction, an overlapping-photon event usually has one  $\pi^0$  photon near the  $\pi^+$  direction and the other in the opposite direction. Events were accepted if the constrained kinematic fit satisfied  $P(\chi^2) > 0.1$ . At this point, the background with a photon escape was estimated to be less than one event.

Remaining background events were primarily due to  $K_{\pi 3}$  and  $K_{\pi 2\gamma}$  decays with multiple photons fused in the barrel calorimeter to form a single cluster. Background with overlapping clusters was greatly reduced by rejecting events with cluster shapes inconsistent with that

of a single photon. A typical single photon cluster contained 4 – 5 hit modules in the barrel calorimeter. The maximum discrepancy among  $z$  measurements and the standard deviation of  $\phi$  measurements were calculated for each photon cluster, and events were rejected if one of the cut variables exceeded the 72% acceptance point. The acceptance was measured using a clean single-photon cluster based on  $K_{\pi 2}$  data with the same number of hit elements and a similar energy. A total of 31  $K^+ \rightarrow \pi^+ \gamma \gamma$  decay candidates survived all the cuts (Fig. 1). The residual background was estimated by measuring the rejections of the  $z$  and  $\phi$  cuts. Each cut was inverted to enhance the overlapping-cluster background, and the rejection of the other cut was evaluated by assuming the two cuts were independent. The independence of the cuts and the magnitude of the background level were confirmed by a large statistics Monte Carlo simulation. The estimated number of the total background was  $5.1 \pm 3.3$ .

The acceptance was estimated by using Monte Carlo simulation and calibration data sets. The net acceptance for the  $\pi \gamma \gamma 1$  trigger and analysis was  $(1.5 \pm 0.2) \times 10^{-4}$  which included a factor 0.12 for the  $\pi^+$  momentum being between 215 MeV/ $c$  and the end point 227 MeV/ $c$  assuming the phase-space distribution. Under this assumption, the 90% C.L. upper limit was  $B(K^+ \rightarrow \pi^+ \gamma \gamma, \text{phase-space distribution}) < 5.0 \times 10^{-7}$ .

The momentum dependence of the  $\pi \gamma \gamma 2$  acceptance is shown in Fig. 1 together with the final  $\pi \gamma \gamma$  candidates and the estimated background spectrum. A partial branching ratio for each 10-MeV/ $c$  bin was calculated from the background-subtracted signal divided by the number of the stopped kaons times the acceptance for that bin. By summing these, a model-independent branching ratio  $B(K^+ \rightarrow \pi^+ \gamma \gamma, 100 \text{ MeV}/c < P_{\pi^+} < 180 \text{ MeV}/c)$  was obtained to be  $(6.0 \pm 1.5 \pm 0.7) \times 10^{-7}$  where the first uncertainty is statistical and the second is the estimated systematic uncertainty in the background and the acceptance measurements based on a  $K_{\pi 2}$  branching ratio measurement.

The measured  $\pi^+$  spectrum was compared with ChPT predictions integrated over 10-MeV/ $c$  bins. A maximum likelihood fit of  $\hat{c}$  to the spectrum using the absolutely-normalized rate was carried out to determine the value of  $\hat{c}$ . Without the unitarity corrections, the result was  $\hat{c} = 1.6 \pm 0.6$  with  $\chi^2_{min.} = 6.3$  ( $n.d.f. = 7$ ). With the corrections, the best fit was obtained for  $\hat{c} = 1.8 \pm 0.6$ , and the  $\chi^2_{min.}$  improved to 4.6. Thus, the data support the inclusion of the unitarity corrections. If we fit the spectrum shape alone by introducing one free normalization factor, the fits became equally good, with  $\chi^2_{min.}/n.d.f. \sim 0.7$ . The corresponding  $\hat{c}$  was  $-0.6^{+1.4}_{-1.1}$  and  $0.7^{+1.7}_{-1.1}$  for without and with the unitarity corrections, respectively. Fig. 2 shows the measured momentum spectrum together with the spectrum shape given by the best fit (*i.e.*  $\hat{c} = 1.8$  with the unitarity corrections). By assuming this spectrum shape, a total branching ratio was estimated to be  $(1.1 \pm 0.3 \pm 0.1) \times 10^{-6}$  with the net acceptance in the  $\pi \gamma \gamma 2$  region being  $3.8 \times 10^{-4}$ . The total branching ratio estimated with a spectrum shape given by the other fits was within 11 % of the above value.

One of the consequences of the unitarity corrections is a non-zero amplitude at the end point  $P_{\pi^+} = 227 \text{ MeV}/c$  ( $m_{\gamma \gamma} = 0 \text{ MeV}/c^2$ ). However, the predicted decay rate at the end point is 8 times smaller than our 90% C.L. upper limit in this region,  $B(K^+ \rightarrow \pi^+ \gamma \gamma, P_{\pi^+} > 215 \text{ MeV}/c) = 6.1 \times 10^{-8}$ , as shown in Fig. 2. Therefore, the ChPT prediction with the unitarity corrections is consistent with our  $\pi \gamma \gamma 1$  result.

The  $\pi \gamma \gamma 1$  result also sets a 90 % confidence upper limit on  $B(K^+ \rightarrow \pi^+ X^0, X^0 \rightarrow \gamma \gamma)$ , where  $X^0$  is any short-lived neutral particle with a mass smaller than 100 MeV/ $c^2$  decaying into two photons. Fig. 3 shows the limit as a function of  $M_{X^0}$  for different lifetimes.

## ACKNOWLEDGMENTS

We gratefully acknowledge the dedicated efforts of the technical staff supporting this experiment and of the Brookhaven AGS Department. This research was supported in part by the U.S. Department of Energy under contracts DE-FG02-91ER40671, W-7405-ENG-36, and grant DE-FG02-91ER40671, and by the Natural Sciences and Engineering Research Council, by the National Research Council of Canada, and by the Ministry of Education, Science, Sports and Culture of Japan.

## REFERENCES

- (*a*) Present address: Research Center for Nuclear Physics, Osaka University, Ibaraki, Osaka 567, Japan.
  - (*b*) Present address: The Conac Group, Richmond, BC, Canada.
  - (*c*) Deceased.
  - (*d*) Present address: Department of Physics, Case Western Reserve University, Cleveland, OH 44106.
  - (*e*) Present address: Princeton Consultants, Inc., Princeton, NJ 08540.
  - (*f*) Present address: Stanford Linear Accelerator Center, Stanford, CA 94309.
  - (*g*) Present address: Thomas Jefferson National Accelerator Facility, Newport News, VA 23606.
  - (*h*) Present address: CERN, CH-1211, Genève 23, Switzerland.
  - (*i*) Present address: Loomis Laboratory of Physics, University of Illinois, Urbana, IL 61801.
  - (*j*) Present address: Institute of Particle and Nuclear Studies (IPNS), High Energy Accelerator Research Organization (KEK), Tsukuba, Ibaraki 305, Japan.
  - (*k*) Present address: Physics Department, Rice University, Houston, TX 77005.
  - (*l*) Present address: Physics Department, University of Colorado, Boulder CO 80309.
  - (*m*) Present address: Enrico Fermi Institute and Physics Department, University of Chicago, Chicago, IL 60637.
- [1] J.F. Donoghue, E. Golowich, and B.R. Holstein, *Dynamics of the Standard Model*, (Cambridge University Press, Cambridge, 1992), and references therein.
  - [2] G. Ecker, A. Pich, and E. de Rafael, Nucl. Phys. **B303**, 665 (1988).
  - [3] G. Ecker, A. Pich, and E. de Rafael, Phys. Lett. B **237**, 481 (1990).
  - [4] H.Y. Cheng, Phys. Rev. D **42**, 72 (1990).
  - [5] C. Bruno and J. Prades, Z. Phys. C **57**, 585 (1993).
  - [6] G. Ecker, J. Kambor, and D. Wyler, Nucl. Phys. **B394**, 101 (1993).
  - [7] G.D. Barr *et al.* (CERN-NA31), Phys. Lett. B **284**, 440 (1992).
  - [8] V. Papadimitriou *et al.* (FNAL-E731), Phys. Rev. D **44**, R573 (1991).
  - [9] L. Cappiello, G. D'Ambrosio, and M. Miragliuolo, Phys. Lett. B **298**, 423 (1993).
  - [10] A.G. Cohen, G. Ecker, and A. Pich, Phys. Lett. B **304**, 347 (1993).
  - [11] G. D'Ambrosio and J. Portolés, Phys. Lett. B **389**, 770 (1996).
  - [12] M.S. Atiya *et al.*, Phys. Rev. Lett. **65**, 1188 (1990).
  - [13] M.S. Atiya *et al.*, Nucl. Instrum. Methods Phys. Res., Sect A **321**, 129 (1992).
  - [14] S. Adler, Ph.D. thesis, State University of New York at Stony Brook, 1995 (unpublished).

# FIGURES

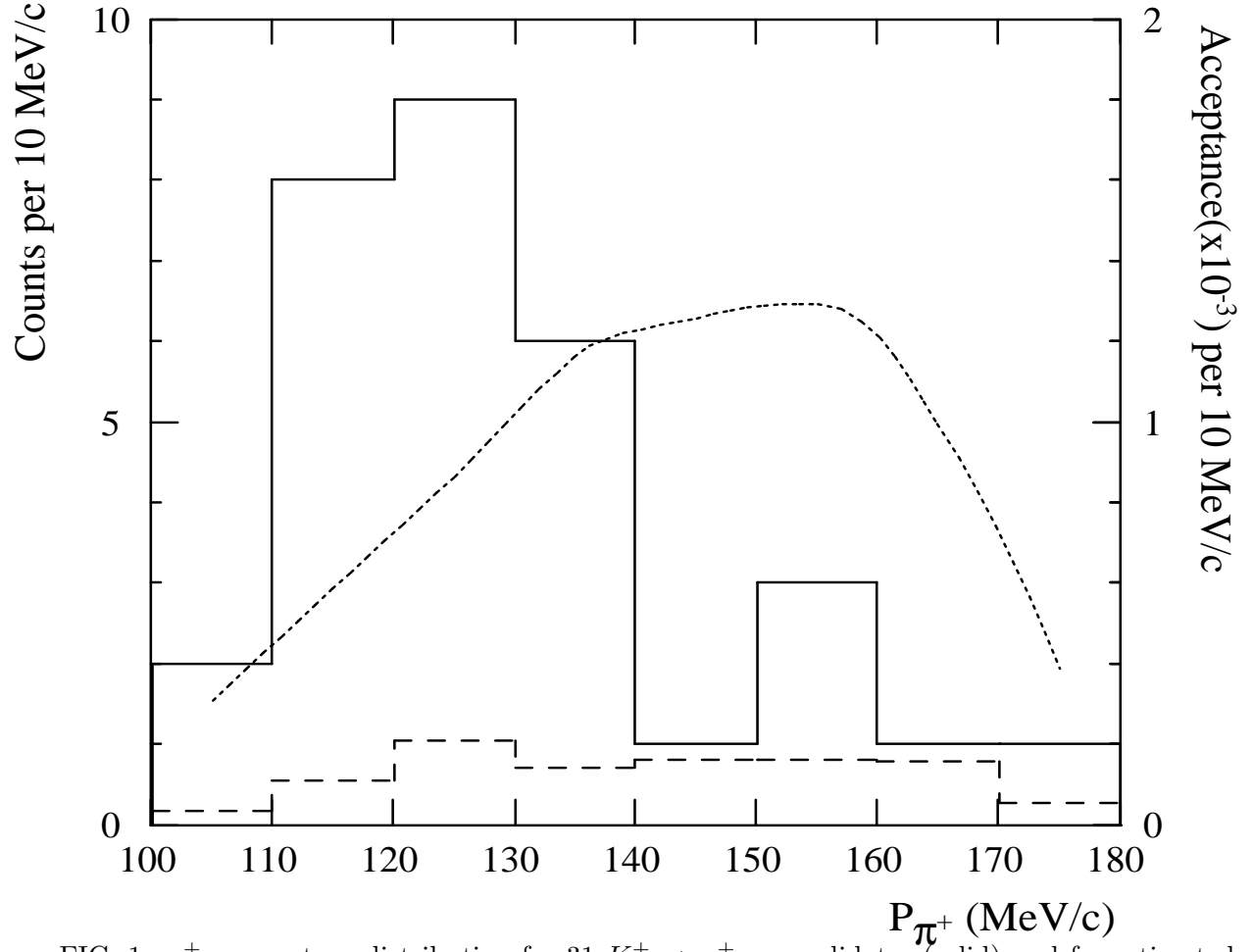


FIG. 1.  $\pi^+$  momentum distribution for 31  $K^+ \rightarrow \pi^+ \gamma \gamma$  candidates (solid) and for estimated background events (dashed). The acceptance is given by the dotted line.

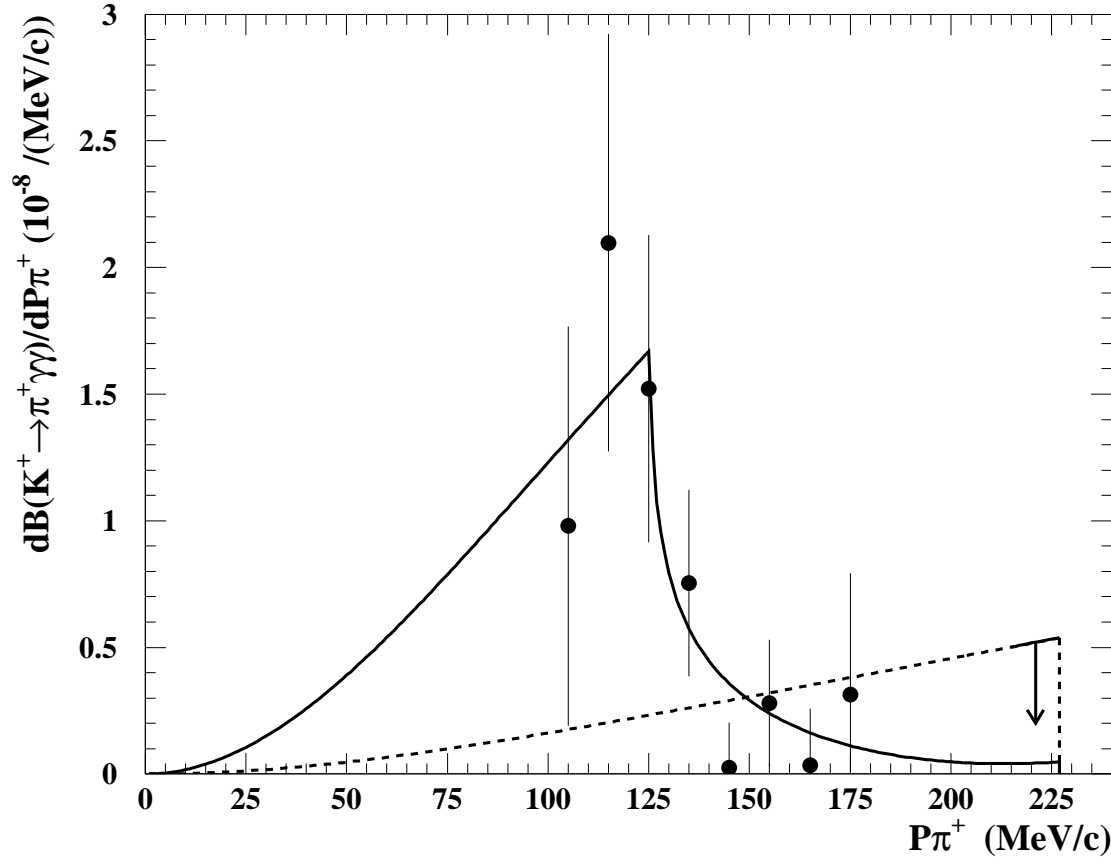


FIG. 2. Measured  $\pi^+$  momentum distribution for  $K^+ \rightarrow \pi^+ \gamma \gamma$  and the best fit to the data (solid). The dashed line shows a phase-space distribution normalized to a 90% C.L. upper limit obtained by the  $\pi \gamma \gamma 1$  analysis in the region of  $215 \text{ MeV}/c < P_{\pi^+} < 227 \text{ MeV}/c$  indicated by the arrow.



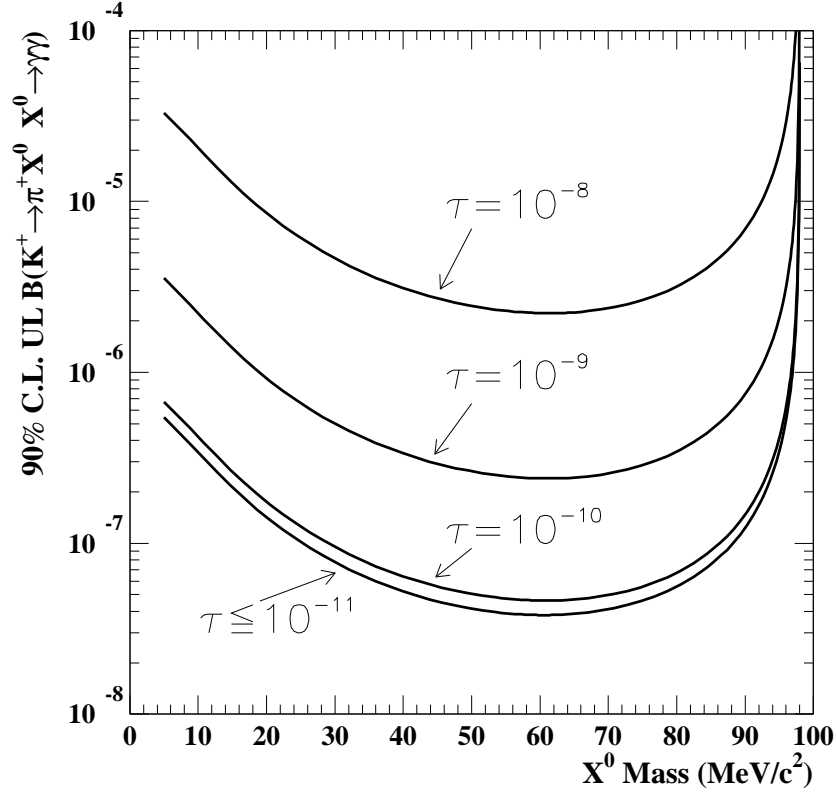


FIG. 3. The 90% C.L. upper limits for the branching ratio of  $K^+ \rightarrow \pi^+ X^0, X^0 \rightarrow \gamma\gamma$  for different  $X^0$  lifetimes ( $\tau_{X^0}$ ) as a function of mass ( $m_{X^0}$ ).